Journal of Applied Polymer Science

Synthesis, Characterization, and *In Vitro* Biocompatibility Study of Novel Disulfide Cross-Linked Hydrogels Based on Poly(amic acid)

Kun Peng,[1,2] Jiaoxia Sun,[1,3] Yuanliang Wang,[1] Yuxiao Li,[1] Bingbing Zhang,[1] Bin Wang[1]

[1]Key Lab of Biorheological Science and Technology, Research Center of Bioinspired Material Science and Engineering, College of Bioengineering, Chongqing University, Chongqing 400030, China

[2]Department of Medical Technology, Chongqing Medical and Pharmaceutical College, Chongqing 401331, China

[3]School of River and Ocean Engineering, Chongqing Jiaotong University, Chongqing 400074, China

Correspondence to: Y. Wang (E-mail: wyl@cqu.edu.cn)

ABSTRACT: In this study, novel disulfide cross-linked hydrogels were designed and synthesized. First, ethylenediaminetetraacetic dianhydride reacted with butanediamine and amino-terminated polyethylene glycol via *N*-acylation reaction to give biocompatible poly(amic acid) (PAA) with pendant carboxyl groups; then, the amino groups of cystamine reacted with carboxyl groups of PAA to generate disulfide cross-linked network polymer (PAA-SS). Fourier transform infrared spectroscopy, ^{1}H nuclear magnetic resonance imaging, gel permeation chromatography with multiangle laser light scattering, potentiometric titration, rheology, hydrolytic degradation, morphology, porosity, and *in vitro* biocompatibility studies were used to qualitatively and quantitatively characterize the obtained polymers. The results indicated that the equilibrium swelling ratio of the PAA-SS decreased with the increase in Rm. The PAA-SS provided good mechanical strength to maintain their integrity, and the storage modules (G') of the hydrogels can be adjusted by Rm. The PAA-SS presented co-continuum pores, and the pore size correlated with the cross-linking degree. The degradation of PAA-SS could be controlled by regulating the concentration of dithiothreitol. Particularly, the PAA-SS possessed an excellent biocompatibility, as the average proliferating rate of osteoblasts on PAA-SS was appreciably higher than that on PAA and glass coverslips. In conclusion, the above obtained results demonstrate that the performance of the PAA-SS outbalance and facilitate the application in biomedical region, particularly in bone tissue regeneration. © 2014 Wiley Periodicals, Inc. J. Appl. Polym. Sci. **2014**, *131*, 40930.

KEYWORDS: biocompatibility; biodegradable; biosynthesis of polymers; copolymers; functionalization of polymers

Received 22 November 2013; accepted 23 April 2014

DOI: 10.1002/app.40930

INTRODUCTION

Hydrogels, due to their high water affinity, permeability, and molecular diffusivity, are suitable for biomedical region, including as drug delivery carriers or as scaffold for tissue engineering.[1–3] Most studied hydrogels fall into three categories: synthetic, natural, and hybrid ones. Among them, the synthetic hydrogels possess a tunable chemical composition and three-dimensional physical structure that enable to control mechanical properties, biodegradation, and biocompatibility.[4,5] The hydrophilic multifunctional polymers that contain reactive groups are commonly used to form cross-linked hydrogel. In our previous study, we synthesized a novel pH-sensitive hydrogel based on hydrophilic multifunctional poly(amic acid) (PAA), polyamide prepolymer with pendant carboxyl groups (PEB-COOH) and amino-terminated polyethylene glycol (ATPEG).[6] PAA can be prepared using bifunctional anhydride and diamine by polycondensation reaction. Aromatic PAA is commonly obtained as an intermediate product when synthesizing polyimide.[7–10] Recently, aliphatic PAA was exposed to biomaterial region for its multifunction and potential biocompatibility. Padavan et al.[11–13] synthesized a PAA graft/cross-linked poly(vinyl alcohol) hydrogel to improve the mechanical property of poly(vinyl alcohol), and they also evaluated the biocompatibility of PAA.

Biodegradation of a hydrogel is considered a critical requirement for its use as biomaterial.[14,15] In this study, combining the advantages of multifunction and biocompatibility of aliphatic PAA, we aimed to prepare a controllable biodegradation hydrogel based on aliphatic PAA. First, a novel aliphatic PAA was synthesized and then cross-linked by disulfide bond. Compared with our previously prepared PAA, i.e., PEB-COOH,[6] PEG

This article was published online on 16 May 2014. An error was subsequently identified. This notice is included in the online and print versions to indicate that both have been corrected 09 June 2014.

sequences were introduced into the polymer main chain. The introduced PEG sequences could reduce interfacial free energy and improve PAA molecule number and biocompatibility. Hydrogels cross-linked with disulfide bonds that can be cleaved and re-cross-linked have been reported. They can swell or completely dissolve once the disulfide bonds are cleaved by reducing reagents such as dithiothreitol (DTT), *N*-acetyl-cysteine, or glutathione.[16–18] In the previous study, we have performed preliminary research on the degradation of the disulfide bonds and PEG cross-linked PAA hydrogels.[19] In this research, the structure of PAA and hydrogels are characterized in detail. Mechanical properties and swelling behavior of hydrogels with different cross-link density were determined. The hydrolytic degradation of hydrogels was extensional examined with or without DTT. The biocompatibility of hydrogels was also studied *in vitro*.

EXPERIMENTAL

Materials

Ethylenediaminetetraacetic dianhydride (EDTAD, 98%), butanediamine (BDA, 99%), cystamine di-HCl (98%), *N*-hydroxy-succinamide (98%), DTT (99%), 1-(3-dimethylaminopropyl)-3-ethylcarbodiimide hydrochloride (98%), and ATPEG500 with a relative molecular weight (Mr) of 600 were purchased from Sigma-Aldrich Corp. Dimethylsufoxide (DMSO) and acetoacetate were of analytical grade from Chongqing Drug Stock Co. Before use, 500 mL DMSO was dried with 100 g activated 4 Å molecular sieve for 24 h. Methylthiazolyl tetrazolium (MTT) was supplied by Sigma-Aldrich Corp. Dulbecco's modified Eagle's medium (DMEM)/F12, trypsin, and fetal bovine serum were purchased from Gibco.

Synthesis of Hydrogel

Synthesis of PAA. First, BDA and ATPEG500 of molar ratio 2 : 1 were added into DMSO. After stirring 2 min, dried EDTAD powder was poured into the mixture. The reaction lasted for 24 h at 25°C under nitrogen protection. Then, the mixture was added dropwise into excessive acetoacetate to produce precipitates. The filtered precipitates were washed with acetoacetate for three times, and subsequently vacuum dried to constant weight at 40°C to give purified products.

Synthesis of PAA-SS. One gram dried PAA (corresponding to about 2.94 mmol —COOH groups) was dissolved in a beaker containing 15 mL DMSO with a magnetic stirring bar. Then 0.3 g *N*-hydroxy-succinamide and 0.6 g 1-(3-dimethylaminopropyl)-3-ethylcarbodiimide hydrochloride were added. The resulting mixture was continuously stirred for 10 min; subsequently, a predetermined amount of cystamine di-HCl was added. The obtained mixture was immediately poured into a glass mold. The cross-linking reaction in DMSO was allowed to last for 24 h at room temperature. Afterward, they were immersed in distilled water that was refreshed. Finally, the swollen hydrogels were lyophilized for 24 h, producing the desired network polymer, i.e., PAA-SS. In order to evaluate the effect of cross-linker on hydrogel properties, various molar ratios of cystamine di-HCl to —COOH (Rm), i.e., Rm = 0.4, 0.6, 0.8, and 1.0 were used and referred as PAA-SS Rm, where Rm varies.

Characterization of Hydrogels

Fourier transform infrared (FTIR) spectroscopy spectra were recorded on a Perkin Elmer Spectrum GX model using the KBr disk method. ^{1}H nuclear magnetic resonance (^{1}H NMR) imaging spectra were recorded at 500 MHz on a Bruker AV-500 nuclear magnetic resonance spectrometer with Bruker software. Samples of about 40 mg were dissolved in dimethyl sulfoxide-*d*6 (Fluka Chemical, deuteration degree not less than 99.8%).

The number–average molecular weights (M_n), the weight–average molecular weights (M_w), and the polydispersity index were determined from gel permeation chromatography (GPC) with multiangle laser light scattering (laser photometer Dawn EOSTM, Wyatt Technology Corp., USA).

Potentiometric Titration Experiment

The carboxyl residual rate was estimated by potentiometric titration based on the idea mentioned in the work of Liu et al.[20] The accurately weighed hydrogels were dissolved in hydrochloric acid solution (0.1*M*) with magnetic stirring bar for 4 h, and the calculated amount of NaCl (0.1*M*) was added to maintain the ionic strength. A standard solution of NaOH and NaCl, both 0.1*M*, was used as the titrant. Alkalimetric curves were recorded by a ZDJ-4A automatic titrator equipped with E-201-C-65 pH electrode. Three replicates were performed for each sample. The following formulae were proposed to calculate the carboxyl residual ratio of hydrogels:

$$\text{Carboxyl residual ratio } (\%) = (V_4 - V_3)/(V_2 - V_1) \times 100\%$$

where, V_1 is the volume of sodium hydroxide consumed by excessive hydrochloric acid of PAA; V_2 is the volumes of sodium hydroxide corresponding to titration terminal of —COOH of PAA; V_3 is the volume of sodium hydroxide consumed by excessive hydrochloric acid of hydrogels; and V_4 is the volumes of sodium hydroxide corresponding to titration terminal of —COOH of hydrogels.

Rheology

The rheological measurements were performed by a rheometer (Gemin HR Nano, Malvern) with cone plate geometry at 37°C and plate diameter of 40 mm.[21,22] The hydrogel samples were equilibrated on the plate for 5 min to reach the running temperature before each measurement. The strain sweep test was performed at a constant frequency of 1 Hz with percentage strain ranging from 10^{-1} to 20. All the rheological studies were done in triplicate, and the average value was reported.

Test of Swelling Kinetics

For swelling kinetics studies, the dried hydrogel samples were immersed in phosphate-buffered saline (PBS) at 37°C for a predetermined time, and then wiped with moistened filter paper and weighed. The swelling ratio (SR) was calculated from the following equation:

$$\text{SR} = (W_s - W_d)/W_d$$

where, W_d and W_s were the weights of dried and swollen hydrogels, respectively.

Study of Hydrolytic Degradation

The lyophilized PAA-SS was immersed in PBS at room temperature for 24 h. The different concentration of DTT/PBS solution

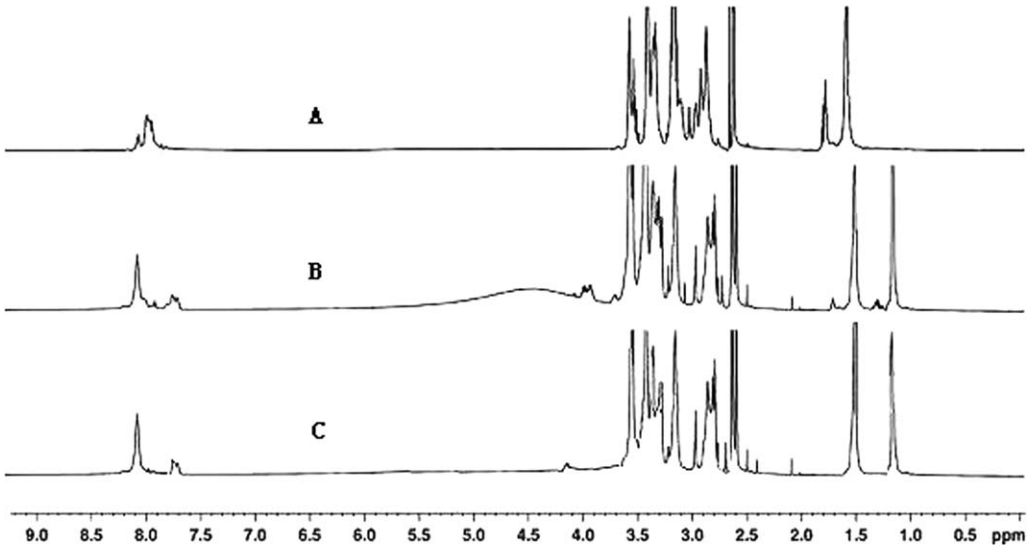

Figure 1. ^{1}H NMR of PEB-COOH[6] (A), PAA (B), and PAA-SS (C).

was then added. At a given time, the samples were collected and washed with distilled water and then were vacuum dried to constant weight. The weight loss rate was calculated as follows:

$$\text{Weight loss rate } (\%) = (W_0 - W_1)/W_0$$

where, W_0 and W_1 are the weights of samples before and after degradation, respectively.

All the above experiments were carried out in triplicate, and the SRs and weight loss rate were reported as the average of three separate experiments ± SD ($n = 3$).

Study of Morphology

The surface microstructures of the hydrogels were examined by a scanning electron microscopy (SEM). For the measurement, the microspheres were dispersed in ethyl alcohol, and the dispersion was dropped on aluminum foil and dried at ambient atmosphere. The different freeze–dried samples were fractured in liquid nitrogen using a razor blade. Then, the samples were attached to metal stubs, sputter coated with gold under vacuum, and observed using a SEM (Tescan, Czech Republic).

Test of Porosity

The porosity of the hydrogels was measured by mercury intrusion porosimeter (Quantachrome, USA). To determine the porosity, it was assumed that the shape of the pores is cylindrical. The contact angle of mercury is 130°, and the surface tension of mercury is 0.485 N/m.

In Vitro Biocompatibility Study

The osteoblasts were isolated from newborn SD rat calvaria by an established method.[23] Cells were cultured in DMEM/F12 supplemented with 10% fetal bovine serum, 100 U/mL penicillin, and 100 μg/mL streptomycin at 37°C in a humidified atmosphere of 5% CO_2 in air. Culture medium was replaced every 2 days. After reaching 80% confluence, cells were released from the tissue culture flask with trypsin and passaged in new basal medium. The third to fifth passage cells were used for experiments.

The proliferation of cells in different polymer films was determined by MTT assay. Osteoblasts were seeded on PAA and PAA-SS films at a density of 1×10^4 cells/well and cultured in DMEM/F12 supplemented with 10% fetal bovine serum and maintained in a controlled atmosphere (5% CO_2/95% air, 37°C) for 1, 3, 5, and 7 days, respectively. After that, 50 μL MTT solution (5 mg/mL in PBS) was added to each sample and continued to incubate at 37°C for 4 h; the blue formazan reaction product formed was then dissolved by adding 0.5 mL DMSO. The absorbance was measured at 570 nm using a Bio-Rad 550 spectrophotometric microplate reader. The average proliferating rate of osteoblasts was percentage of the increased osteoblasts quantity per day, calculated according to the following equation:

$$\text{The average proliferating rate of osteoblasts} = (P_2 - P_1)/\times\ \Delta t$$

in which, P_1 and P_2 are the optical density (OD) values at culture times t_1 and t_2, respectively; Δt is the time interval between P_1 and P_2, that is, $t_2 - t_1$.

Statistical Analysis

One-way single factor analysis of variance was used to analyze the statistical significance of experimental results. Experimental data were expressed as means ± SD ($n = 3$ for all experiments except for cell proliferation experiments $n = 4$), and $P < 0.05$ was considered significant difference.

RESULT AND DISCUSSION

Characterization of Hydrogels

To characterize the structure of PAA, the ^{1}H NMR spectra of polymers are displayed in Figure 1, which showed valuable information on molecular structure. Compared with the spectra of PEB-COOH [Figure 1(A)], the peaks at ~1.5 ppm and at ~3.15 ppm in PAA [Figure 1(B)] were corresponding to the two different protons of —CH_2— in BDA. Meanwhile, the peak at ~1.1 should be assigned to the chemical shift of —CH_3 in ATPEG, which means PEG was successfully introduced into PAA. The peak at ~8.0 ppm was contributed by the protons of

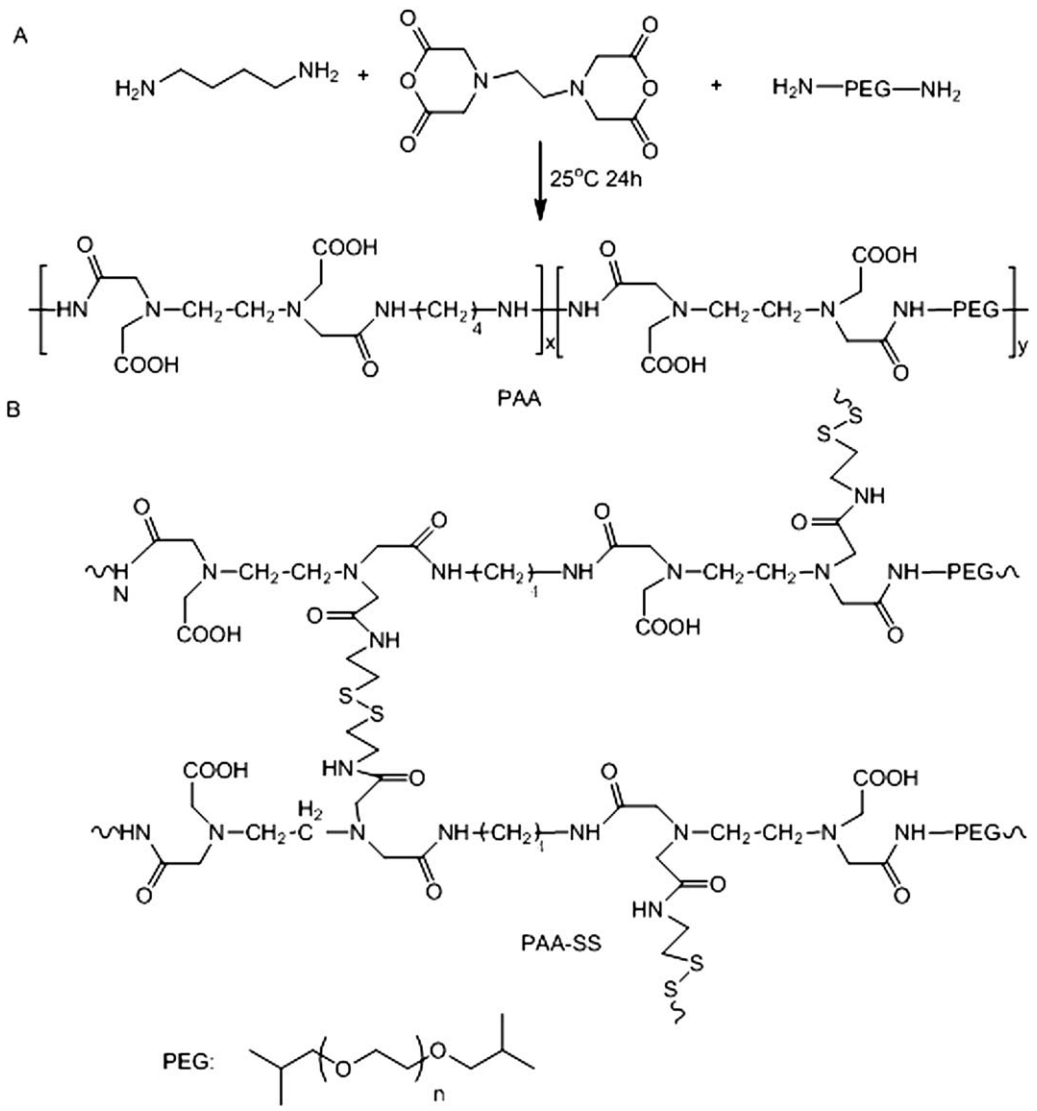

Scheme 1. Synthesis route of PAA (A), and the chemical structure of PAA-SS hydrogel (B).

—CONH— bonds. The existence of —CONH— in the obtained polymer indicated the successful *N*-acylation of the anhydride groups in EDTAD with amino groups in BDA and ATPEG, producing the desired PAA prepolymer PAA as shown in Scheme 1. The peak at ~8.0 ppm was intensified in PAA-SS [Figure 1(C)]. One reason may be that the carboxyl of PAA and amino of cystamine di-HCl formed acylamino by cross-linking reaction.

Figure 2 indicated the FTIR spectra of PAA and PAA-SS 1.0, both of which were used as prepared. In Figure 2(A), typical amide I and II bands were present at ~1658.60 and ~1580.11 cm^{-1}, respectively. The absorption band at ~1719.81 cm^{-1} attributed to C═O of carboxyl groups in PAA. These evidences further verified the successful reaction of EDTAD with BDA and ATPEG. Compared with Figure 2(A), the peak at ~1719.81 cm^{-1} disappeared in Figure 2(B). The reason was that most of the carboxyl groups of PAA were consumed because they reacted with the amino groups of cystamine di-HCl. Furthermore, Figure 2(B) provided a new absorption band at 1039.14 cm^{-1}, which was ascribed to the vibration of C—S—S—C. The disappearance of C═O from carboxyl group and the existence of C—S confirmed that —COOH in PAA reacted with amino group in AET and cross-linked successfully by disulfide.

GPC-multiangle laser light scattering was used to determine the molecular weight of PAA. The GPC separation was carried out by using two TSK-GEL ALPHA-2500 HPLC columns (300 × 7.8 mm) with PBS as the eluent; the temperature was set at 25°C, and the flow rate was 1 mL/min. The solvent was 1,2,4-trichlorobenzene with 400 mg/L Irganox 1010 added in order to stabilize the polymer against oxidative degradation. The MALS detector is equipped with a laser at 690 nm and 17 multiangle detectors. Temperature was also set at 25°C. The photometer system was calibrated with toluene, and the detectors were normalized with a standard monodisperse polystyrene (PS) ($M_w = 30$ kg/mol), which was also used to determine inter-detector volume. The number–average molecular weight (M_n) of PAA is 2×10^4, and polydispersity index = M_w/M_n is 1.42.

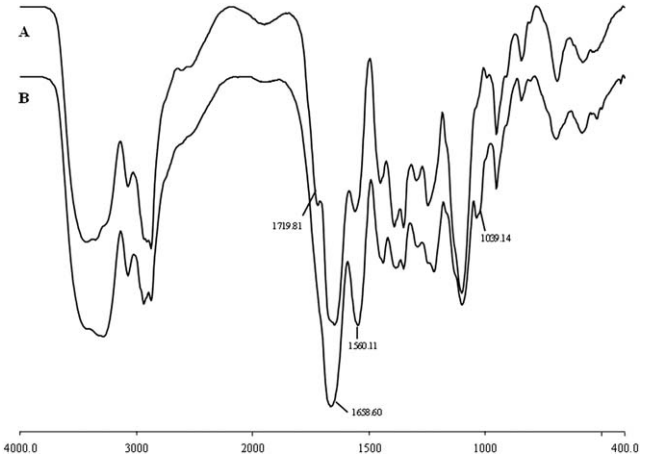

Figure 2. FTIR of PAA (A) and PAA-SS 1.0 (B) hydrogel.

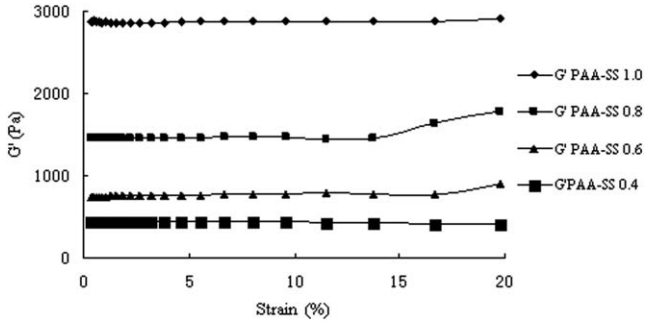

Figure 3. Influence of strain on G' of hydrogels.

The results of carboxyl residual rate are shown in Table I. It obviously indicated that the carboxyl residual ratio of hydrogels decreases as the introduction of Rm increases. Conversely, because carboxyl of hydrogel and amino of cystamine di-HCl could form acylamino by condensation reaction, the degree of cross-linking increases with the decrease in carboxyl residual ratio of hydrogels.

Rheology of Hydrogels

The property of these hydrogels determined their application. In tissue engineering, the stiffness of the implanted material should roughly match that of the tissue it replaces.[24–26] To explore the application of the hydrogels, the mechanical strength and viscoelastic properties of the hydrogels were investigated by rheological measurements. The rheological studies were performed on PAA-SS 0.4, PAA-SS 0.6, PAA-SS 0.8, and PAA-SS 1.0 (Figure 3). The strain sweep test was performed on all the hydrogels in order to establish the range of linear viscoelasitcity and to determine whether the elasticity of the formulations differed as expected by the storage/elastic modulus (G'). The storage modulus of PAA-SS 1.0 reached 2900 Pa. The results suggested that the value of G' increases with the amount of cross-linker increasing, so that the hydrogels could sustain their integrity because of being equipped with good mechanical property.

SR of Hydrogels

The equilibrium SRs and swelling kinetics were performed in PBS at 25°C. Figure 4 illustrated that the swelling kinetics of hydrogels are expressed as a function of SR against immersion time of the hydrogel. The hydrogels in this study reached equilibrium swelling after immersing in PBS for 10 h. At the same time, with the increase in cross-linking density, SR decreased. The SR of PAA-SS 1.0 reached about 18 and that of PAA-SS 0.4 was about 10. These results demonstrated, as expected, that the cross-linking density was inversely proportional to the degree of swelling.

Usually, the swelling process is complicated and involves three successive steps[27]: (1) diffusion of water molecules into a polymer system, (2) the subsequent relaxation of hydrated polymer chains, and (3) the expansion of polymer network into aqueous solution. In this study, Steps 2 and 3 induced the different swelling rates. The swelling was related to the mechanical relaxation of the coiled polymeric chains and the protonation and deprotonation of amino and carboxyl groups in the hydrogel. The PEG introduced in to the polymer chain makes it highly hydrophilic. The major difference of PAA-SS 1.0, PAA-SS 0.8, PAA-SS 0.6, and PAA-SS 0.4 can be attributed to the degree of cross-linking. When the degree of cross-linking was increased, the relaxation of polymer chains would be restricted and the amount of the unreacted carboxyl groups in network decreased with the increase in cystamine di-HCl, which resulted in the electrostatic repulsion between networks reduced. Therefore, the swelling rate of the resulted hydrogel decreased accordingly.

Morphology and Porosity of Hydrogels

The morphology of the swelling hydrogels was observed by SEM (Figure 5). The hydrogels were frozen rapidly by liquid nitrogen and lyophilized instantly. The samples showed a co-continuous open porous structure, and the pore size showed a strong correlation with the cross-linker. The PAA-SS 0.4 and 0.6 present loose porous structure. The pore size of hydrogels

Table I. Carboxyl Residual Ratio of Hydrogels by Potentiometric Titration Experiments

Samples	V_1	V_2	V_3	V_4	Carboxyl residual ratio (%)
PAA	9.05 ± 0.12	13.61 ± 0.17	-	-	-
PAA-SS 0.4	-	-	11.13 ± 0.15	13.98 ± 0.11	62.52 ± 0.65
PAA-SS 0.6	-	-	11.37 ± 0.12	13.27 ± 0.07	41.66 ± 0.39
PAA-SS 0.8	-	-	12.16 ± 0.14	13.51 ± 0.09	29.60 ± 0.47
PAA-SS 1.0	-	-	13.02 ± 0.09	13.63 ± 0.13	13.37 ± 0.54

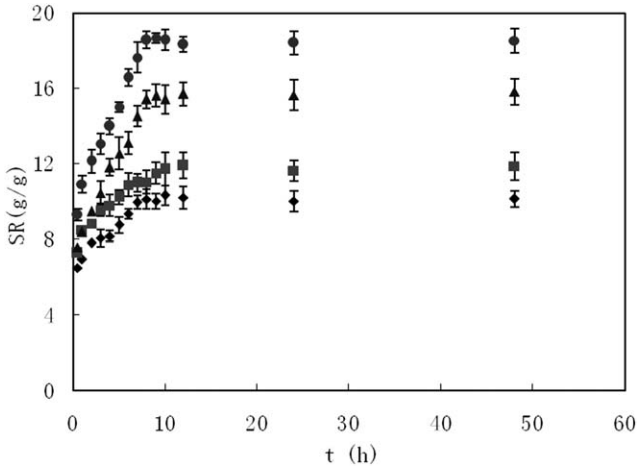

Figure 4. The swelling ratio of hydrogels: PAA-SS 0.4 (◆), PAA-SS 0.6 (■), PAA-SS 0.8 (▲), and PAA-SS 1.0 (●).

shrinks by increasing the density of cross-linking. The discrepancy of pores also corresponded to the variation in mechanical property and SR of the hydrogels, that is, the loose porous structure of hydrogel corresponded to the low mechanical property and high SR and *vice versa*.

The porosity of hydrogels is presented in Table II. It was observed that various molar ratios of cystamine di-HCl to —COOH (Rm = 0.4 and 0.6) did not noticeably change the porosity. However, once the Rm increased to 1.0, the porosity of hydrogel apparently decreased. This finding is in agreement with the results of SEM observation.

Degradation of Hydrogels

Two kind of cleavable bonds, amide bonds and disulfide bonds, in the PAA-SS resulted in two degradation mechanisms. The disulfide cross-linkage (—S—S—) could be cleaved to the thiol groups (—SH HS—) in presence of reducing agents, DTT. The amide bonds enabled to be hydrolyzed in the aqueous solution.

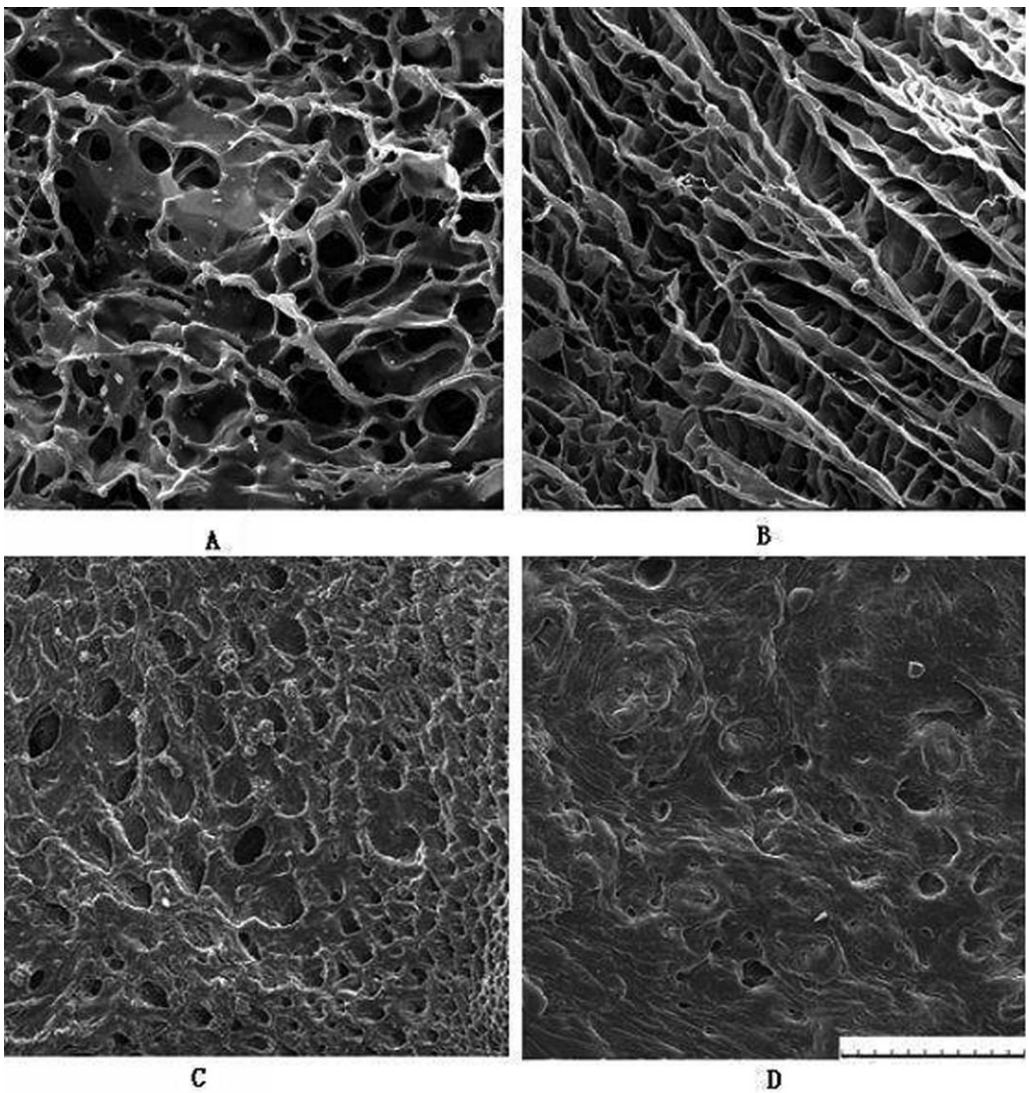

Figure 5. SEM micrographs of hydrogels: PAA-SS 0.4 (A), PAA-SS 0.6 (B), PAA-SS 0.8 (C), and PAA-SS 1.0 (D). White bar is 100 μm.

Table II. Porosity of Hydrogels with Different Cystamine Di-HCl Contents

Samples	Porosity (%)
PAA-SS 0.4	81.10
PAA-SS 0.6	75.22
PAA-SS 0.8	59.51
PAA-SS 1.0	39.34

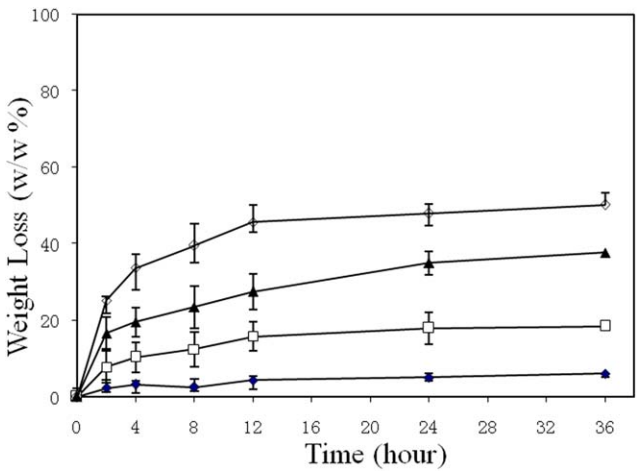

Figure 6. The degradation of PAA-SS 1.0. The concentration of DTT solution is 0 m*M* (◆), 5 m*M* (□), 10 m*M* (▲), and 15 m*M* (◇).

However, with the presence of reducing agents, the disulfide bonds were cleaved quickly. It was expected that the degradation rate of the PAA-SS could be controlled by adjusting the molar ratio of the disulfide bond in PAA-SS and DTT concentration. In this research, we controlled the amount of disulfide bond and changed the concentration of DTT. 0.1 g PAA-SS 1.0 was swollen to reach equilibrium. Then, the swollen PAA-SS 1.0 was immersed into 5 mL 0, 5, 10, and 15 m*M* DTT PBS/solution, respectively. The degradation profile of the cross-linked PAA-SS 1.0 is shown in Figure 6. Without DTT, the degradation of the PAA-SS 1.0 was slow because the hydrolysis of amide bond predominated in this situation, and the hydrolysis rate is tardy. However, when the PAA-SS 1.0 was incubated in DTT solution, the rate of degradation was accelerated with increasing the concentration of DTT during the first 12 h of degradation. The reason is that the cleavage of disulfide bond is associated with the concentration of reducing reagent.[16,17] The controlled degradation of the PAA-SS makes it have potential application in drug delivery or tissue regeneration.

In Vitro Biocompatibility Study

The proliferation of osteoblasts on the two polymer films and glass coverslips is shown in Figure 7. Cell number was increased on the two polymer films and glass coverslips during 7 days of culture. It can be seen that the osteoblasts spread out well and adhered to both the PAA and PAA-SS 0.6 films over 1 day, indicating that both PAA and PAA-SS 0.6 had adequate adhesion surface. The viability determined with the MTT assay measures cell metabolism and provides an indirect correlation of cell proliferation.[28] Cell viability of osteoblasts seeded on the two polymer films was greater than that seeded on glass coverslips ($P < 0.05$).

The results of the average proliferating rate of osteoblasts cultured on the two polymer films and glass coverslips are shown in Figure 8. Because polymer materials have different surface morphology and chemical structure, osteoblasts seeded on different polymer materials needed time to adapt to the new environment.[29] In 1–3 days, osteoblasts in adapting period mainly expressed on anchorage, adhesion, and spread; consequently, the average proliferating rate was slow. In 3–5 days, the average proliferating rate of osteoblasts significantly increased and reached maximum. In 1–5 days, the average proliferating rate of osteoblasts cultured on PAA-SS was appreciably higher than that on PAA and glass coverslips. The results revealed that the co-continuous open porous structure of PAA-SS could improve osteoblasts proliferation. One reason may be that the disulfide-containing PAA-SS enhanced the adhesion of osteoblasts with brushed architecture, as also observed in previous studies.[30,31] The other reason for the lower cytotoxicity of PAA-SS may be that PAA-SS possessed more hydrophilic amide bond than PAA and glass coverslips, which lead to the better cell development environment.[32]

After 5 days, the average proliferating rate of cells on the two polymer films and glass coverslips was significantly reduced. This phenomenon can be explained by the contact inhibition raised from the large osteoblasts density. This visual appearance of osteoblasts on the grafted hydrogel was consistent with

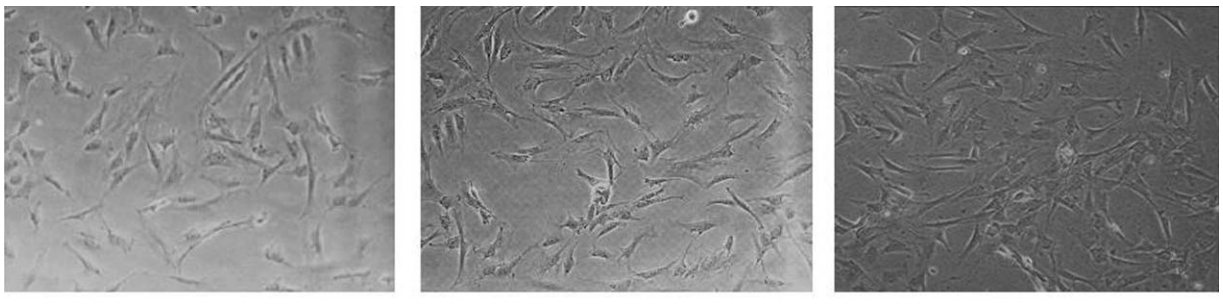

Figure 7. The proliferation of osteoblasts on the two polymer films and glass coverslips. Glass coverslips (A), PAA (B), and PAA-SS 0.6 (C).

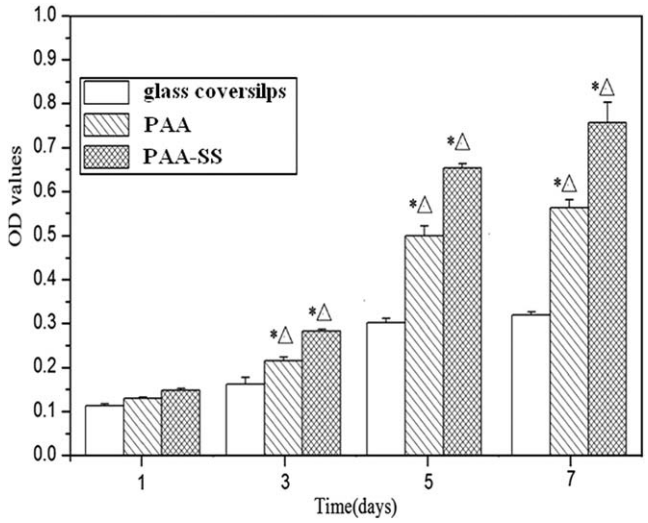

Figure 8. The proliferation of osteoblasts on different materials. The data are the means ± SD for $n = 4$. $^*P < 0.05$ compared with glass coversilps; $\triangle P < 0.05$ compared with PAA.

Padavan et al.'s works,[11–13] in which we demonstrated that PAA-SS is not cytotoxic to cells.

CONCLUSION

Novel hydrogels combining advantages of biocompatibility and controllable degradation have been designed and prepared using EDTAD, BDA, ATPEG500, and cystamine di-HCl as the main feed stock. The results from FTIR and ^{1}H NMR confirmed the successful synthesis of PAA-SS. The results demonstrated that the PAA-SS possessed good mechanical property to sustain their integrity. The elastic modulus could be tailored by changing the degree of cross-linking. The PAA-SS exhibited a decrease in equilibrium SR with the increase in cross-linker. Moreover, the resultant disulfide cross-linked PAA-SS had co-continuum porous network structure and good water-containing capability. The degradation speed of the PAA-SS can be adjusted by varying with the concentration of DTT. The synthetic PAA-SS based on PAA integrated such advantages as tunable degradation, proper mechanical property, and biocompatibility, which provided an alternative material for biomedical application.

ACKNOWLEDGMENTS

This study was supported by the National Natural Science Foundation of China (grant No. 11032012), Natural Science Foundation of The Chongqing Education Committee (grant No. KJ112501), and Natural Science Foundation of Chongqing Health Bureau (grant No. 2012-2-257).

REFERENCES

1. Lee, K.; David, J. *Chem. Rev.* **2001**, *101*, 1869.
2. Lutolf, M. P. *Biomaterials* **2009**, *8*, 451.
3. Piyush Gupta K. V.; Garg, S. *Drug Discov. Today* **2002**, *7*, 569.
4. Lin, C.; Metters, A. *Adv. Drug Delivery Rev.* **2006**, *58*, 1379.
5. Drury, J. *Biomaterials* **2003**, *24*, 4337.
6. Luo, Y. F.; Peng, H.; Wu, J. C.; Sun, J. X.; Wang, Y. L. *Eur. Polym. J.* **2011**, *47*, 40.
7. Kazuhiro, Y.; Mitsutoshi, J.; Masa-Aki, K. *Macromolecules* **2000**, *33*, 6937.
8. Naoki, A.; Kenji, M.; Masahiro, W. *Chem. Mater.* **2004**, *16*, 2841.
9. Tomikawa, M.; Yoshida, S.; Okamoto, N. *Polym. J.* **2009**, *41*, 604.
10. Kawakami, H.; Nagaoka, S.; Kubota, S. *ASAIO J.* **1996**, *42*, M871.
11. Padavan, D. T.; Wan, W. K. *Mater. Chem. Phys.* **2010**, *124*, 427.
12. Padavan, D. T.; Hamilton, A. M.; Millon L. E.; Boughner D. R.; Wan, W. K. *Acta Biomater.* **2011**, *7*, 258.
13. Padavan, D. T.; Hamilton, A. M.; Boughner, D. R.; Wan, W. K. *J. Biomater. Sci. Polym. Ed.* **2011**, *22*, 683.
14. Martens, P. J.; Bryant, S. J.; Anseth, K. S. *Biomacromolecules* **2003**, *4*, 283.
15. Halstenberg, S.; Panitch, A.; Rizzi, S.; Hall, H.; Hubbell, J. A. *Biomacromolecules* **2002**, *3*, 710.
16. Andac, M.; Plieva, F. M.; Denizli, A.; Galaev, I. Y.; Mattiasson, B. *Macromol. Chem. Phys.* **2008**, *209*, 577.
17. Han, S. C.; He, W. D.; Li, J.; Li, L. Y.; Sun, X. L.; Zhang, B. Y. *J. Polym. Sci. Part A Polym. Chem.* **2009**, *47*, 4074.
18. Becker, A. L.; Zelikin, A. N. Johnston, A. P. R.; Caruso, F. *Langmuir* **2009**, *25*, 14079.
19. Sun, J. X.; Wang, Y. L.; Ruan, C. S.; Dou, S. H. *Adv. Mater. Res.* **2012**, 391, 319.
20. Liu, C. X.; Chen, G. H.; Jin, Z. T. *J. Beijing Univ. Chem. Technol.* **2006**, *31*, 14.
21. Rudraraju, V.; Wyandt, C. *Int. J. Pharm.* **2005**, *292*, 63.
22. Vanderhooft, J. L.; Alcoutlabi, M.; Magda, J. J.; Prestwich, G. D. *Macromol. Biosci.* **2009**, *9*, 20.
23. Robey, P. G.; Ternube, J. D. *Calcif. Tissue Int.* **1985**, *37*, 453.
24. Ghosh, K.; Pan, Z.; Guan, E.; Ge, S.; Liu, Y.; Nakamura, T. *Biomaterials* **2007**, *28*, 671.
25. Engler, A. J.; Sen, S.; Sweeney, H. L.; Discher, D. E. *Cell* **2006**, *126*, 677.
26. Georgesm, P. C.; Miller, W. J.; Meaney, D. F.; Sawyer, E. S.; Janmey, P. A. *Biophys. J.* **2006**, *90*, 3012.
27. Zhang, X. Z.; Sun, G. M.; Wu, D. Q.; Chu, C. C. *J. Mater. Sci. Mater. Med.* **2004**, *15*, 865.
28. Niu, X. F.; Wang, L. Z.; Chen, P. *Chem. Phys.* **2013**, *214*, 700.
29. Niu, X. F.; Feng, Q. L.; Wang, M. B. *J. Control. Release* **2009**, *134*, 111.
30. Xiu, K. M.; Yang, J. J.; Zhao, N. N.; Li, J. S.; Xu, F. J. *Acta Biomater.* **2013**, *9*, 4726.
31. Liu, J.; Xu, Y. L.; Yang, Q. Z.; Li, C.; Hennink, W. E.; Zhuo, R. X.; Jiang, X. L. *Acta Biomater.* **2013**, *9*, 7758.
32. Zhao, L. Z. *Chin. J. Conserv. Dem.* **2007**, *17*, 667.